Quasi-Static Modeling of Human Limb for Intra-Body Communications With Experiments

Sio Hang Pun, Yue Ming Gao, PengUn Mak, Mang I Vai, and Min Du

***Abstract*—In recent years, the increasing number of wearable devices on human has been witnessed as a trend. These devices can serve for many purposes: personal entertainment, communication, emergency mission, health care supervision, delivery, etc. Sharing information among the devices scattered across the human body requires a body area network (BAN) and body sensor network (BSN). However, implementation of the BAN/BSN with the conventional wireless technologies cannot give optimal result. It is mainly because the high requirements of light weight, miniature, energy efficiency, security, and less electromagnetic interference greatly limit the resources available for the communication modules. The newly developed intra-body communication (IBC) can alleviate most of the mentioned problems. This technique, which employs the human body as a communication channel, could be an innovative networking method for sensors and devices on the human body. In order to encourage the research and development of the IBC, the authors are favorable to lay a better and more formal theoretical foundation on IBC. They propose a multilayer mathematical model using volume conductor theory for galvanic coupling IBC on a human limb with consideration on the inhomogeneous properties of human tissue. By introducing and checking with quasi-static approximation criteria, Maxwell's equations are decoupled and capacitance effect is included to the governing equation for further improvement. Finally, the accuracy and potential of the model are examined from both *in vitro* and *in vivo* experimental results.**

***Index Terms*—Body area network (BAN), body sensor network (BSN), home health care system, intra-body communication (IBC), quasi-static model, volume conductor theory.**

I. Introduction

THE research and development in the fields of body area network (BAN) and body sensor network (BSN) have recently drawn increasing attention in both academic and industrial arenas. The driving force originates from the benefit of being able to share information between personal portable devices and sensors on the body. BAN and BSN can facilitate the development of the sophisticated instruments for public security forces, army, and paramedics during life-threatening rescue missions. In the medical field, the health care monitoring systems for chronic disease patients and the elderly are one of the main focuses too. An example of a comprehensive health care system might include all personal metabolic sensors, implantable devices (pacemakers, drug delivery devices, etc.), physical activity monitors, and a high performance central control unit. The system should be capable of monitoring, assessing, logging, and communicating with a central server for recording and performing online medical treatment during an emergency. To achieve health care and monitoring, sensors and devices are required to place at various locations of the human body. Then, a BAN is built to provide connectivity to all the sensors and devices scattered throughout the body. At the same time, the design of the BAN should be efficient under limited resources. It is because the on-body sensors and devices generally have stringent requirements on light weight miniaturization, energy efficiency, and less electromagnetic interference.

To implement the physical layer of the BAN, conventional wireless technologies are not designed for communication range around 1–2 m. Therefore, Zimmerman proposed intra-body communication (IBC) for transmitting information over the human body [1], [2]. The IBC can be used as a technique to network various devices on the human body by utilizing the conducting properties of human tissues. It is typically realized by coupling a small amount of electric current, which is below the safety thresholds, into the human body. The current signal then propagates within the human body and is eventually picked up at a suitable location on or in the human body.

Based on previous research [3]– [5], IBC owns the advantages of low power consumption, reduced electromagnetic radiation, lower interference from external electromagnetic noise, increased security, and increased spectrum efficiency. In addition, the design of the IBC transceiver can effectively reduce the complexity of the sensors. For wearable sensors and devices on the body, IBC that uses the human tissue as the communication channel is more natural and convenient.

In the implementation stage of IBC, two variations have been developed. The capacitive coupling technique is a two-electrode approach [6] and the galvanic coupling technique employs four electrodes [5]. The capacitive coupling technique has a higher channel gain [6] and data rate [7], while the galvanic coupling technique is capable of both on-body and in-body (i.e., implanted) devices [8], [9].

Manuscript received February 14, 2011; revised June 17, 2011; accepted June 21, 2011. Date of publication June 30, 2011; date of current version November 23, 2011. This work was supported by The Science and Technology Development Fund of Macau under Grant 014/2007/A1, Grant 063/2009/A, and Grant 024/2009/A1, the Research Committee of the University of Macau under Grant UL012/09-Y1/EEE/VMI01/FST, Grant RG077/09-10S/VMI/FST, Grant RG075/07-08S/10T/VMI/FST, and Grant RG072/09-10S/MPU/FST, the National Natural Science Foundation of China under Grant 51047001, the Funds of Fujian Provincial Department of Education under Grant JK2010006, and the Funds of Fujian Provincial Department of Science and Technology under Grant 2009I0016.

S. H. Pun, P. U. Mak, and M. I Vai are with the Department of Electrical and Electronics Engineering, Faculty of Science and Technology, University of Macau, Taipa, Macau 999078, China (e-mail: lodge@mail.eee.umac.mo; fstpum@umac.mo; fstmiv@umac.mo).

Y. M. Gao and M. Du are with the College of Physical and Information Engineering, Fuzhou University, Fuzhou 350108, China (e-mail: fzugym@yahoo.com.cn; dm_dj90@163.com).

Color versions of one or more of the figures in this paper are available online at http://ieeexplore.ieee.org.

Digital Object Identifier 10.1109/TITB.2011.2161093

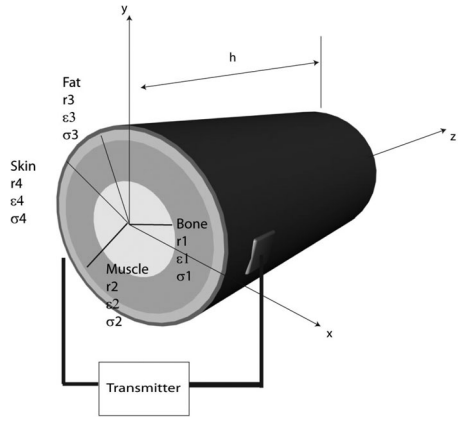

Fig. 1. Representation of IBC limb model ($N = 4$).

Researchers have also applied IBC to a variety of applications. For example, there are prototypes for business card exchange [2], ECG monitoring [3], and virtual typing system [10]. Theoretically, researchers have already examined in various prospectives such as: researches in experiments [11], equivalent-circuit model developments [2], and numerical simulations [12]. However, these empirical approaches can neither provide good explanation to the IBC underlying principle nor establish design criteria for IBC transceiver.

In this paper, the authors propose a multilayer mathematical model based on the volume conductor theory that considers the inhomogeneous properties of human tissues to some extent, for galvanic coupling IBC on a human limb in Section II. By introducing and checking with quasi-static approximation criteria, Maxwell's equations are decoupled and capacitance effect is introduced to the governing equation for improvement. In Sections III and IV, *in vitro* and *in vivo* experiments are described and the results are compared with our model, respectively. Section V gives result discussion and conclusion is made in Section VI.

II. Mathematical Model

Focusing on the galvanic coupling IBC on the upper human arm, which is a convenient site for experiment realization, the model of limb is approximated by a multilayer concentric cylinder. This simplification is analogous to the research of Fujii *et al.* [13], Wegmueller *et al.* [14], Sasamori *et al.* [15], and Oh *et al.* [16]. To elevate the integrity of the model, we have included both permittivities ($\epsilon_1, \ldots, \epsilon_N$) and conductivities ($\sigma_1, \ldots, \sigma_N$) with the geometry illustrated in Fig. 1, where h depicts the length of the limb, and $r_1, \ldots, r_N$ represent the radii of various tissues.

Since the galvanic coupling type IBC generally operated at low frequency, the full-wave formulation of Maxwell's equations was not necessary nor easy to solve. Therefore, we could apply the quasi-static approximation to simplify the IBC problem. In accordance with [17]–[19], we first checked the quasi-static criteria (1)–(4) for potentially decoupling Maxwell's equations

$$\text{Neglect Propagation Effects} \qquad kR_{\max} \ll 1 \tag{1}$$

$$\text{Neglect Capacitance Effects} \qquad \frac{\omega\epsilon}{\sigma} \ll 1 \tag{2}$$

$$\text{Neglect Inductive Effects} \qquad (kR_{\max})^2 \ll 1 \tag{3}$$

$$\text{Neglect Leakage to outside air} \qquad \frac{\omega\epsilon_0}{\sigma_N} \ll 1 \tag{4}$$

where

$$k^2 = \omega^2\mu\epsilon\left(1 + \frac{\sigma}{j\omega\epsilon}\right) \tag{5}$$

and $R_{\max}$ is the maximum length corresponding to the overall dimension of human, ω is the angular frequency, ϵ and σ are the permittivity and conductivity of tissues, ϵ_0 is the permittivity of free space, σ_N is the conductivity of the outmost tissue layer, and μ is the permeability of tissues.

The quasi-static approximation criteria are listed in Table I and calculated using the conductivities and the permittivities of bone, muscle, fat, and skin. The electrical properties of the tissues are derived from the parametric models of Gabriel *et al.* [20] who summarized measurements from *in vivo* experiments on the human body and autopsies of cadavers and animals.

From the table, it is found that except for the capacitance effect of dry skin and wet skin, all other effects are negligible up to 1 MHz. This suggests that the capacitance effect cannot be neglected in the IBC problem within this frequency range. Thus, by including the permittivities of human tissue as suggested by Plonsey and Heppner [17] and applying the quasi-static approximation mentioned in [21], the governing equation for each layer of our multilayer model becomes

$$\nabla \cdot \sigma_{\mathrm{Eq(s)}} \nabla V = 0 \qquad s = 1, \ldots, N \tag{6}$$

$$\sigma_{\mathrm{Eq(s)}} = \sigma_s + j\omega\epsilon_{rs}\epsilon_0 \tag{7}$$

where V represents the potential within the human limb.

The transmission signal of the IBC is then expressed as J_n and the electrode shape can also be introduced into the model by defining

$$\sigma_{\mathrm{Eqn}} \frac{\partial V}{\partial r}\left(r = r_N, \phi, z\right) = J_n\left(\phi, z\right) \tag{8}$$

where $J_n\left(\phi, z\right)$ depicts the normal component of the current density applied to the limb through the side surfaces.

To complete the model, (9) and (10) are required to define the reference potentials of the formulation. Furthermore, for multilayer model, (11) and (12) are necessary for defining the electromagnetic continuity properties across adjacent layers

$$V\left(r, \phi, z = 0\right) = 0 \tag{9}$$

$$V\left(r, \phi, z = h\right) = 0 \tag{10}$$

$$J_{\mathrm{ns}}\left(\phi, z\right) = J_{\mathrm{ns+1}}\left(\phi, z\right) \tag{11}$$

$$V_s\left(\phi, z\right) = V_{\mathrm{s+1}}\left(\phi, z\right) \tag{12}$$

$$s = 1, \ldots, N-1.$$

By solving the mathematical model with (6), (7), (9), and (10), an analytical potential solution for the IBC limb model

TABLE 1
VERIFICATION OF THE QUASI-STATIC CRITERIA

	Frequency (Hz)	Conductivity $\sigma(\mathrm{S/m})$	Relative permittivity ϵ_r	Capacitance effect	Inductive effect	Propagation effect	Leakage to air
Bone	1k	2.00e-2	2.70e3	7.50e-3	6.26e-6	2.50e-3	
	10k	2.00e-2	5.20e2	1.45e-2	6.22e-5	7.89e-3	n/a
	100k	2.1e-2	2.30e2	6.09e-2	6.22e-4	2.49e-2	
	1M	2.4e-2	1.40e2	3.24e-1	5.12e-3	7.15e-2	
Muscle	1k	3.20e-1	4.30e5	7.47e-2	9.34e-5	9.67e-3	
	10k	3.40e-1	2.60e4	4.25e-2	1.03e-3	3.20e-2	n/a
	100k	3.60e-1	8.10e3	1.25e-1	9.94e-3	9.97e-2	
	1M	5.00e-1	1.80e3	2.00e-1	1.26e-1	3.55e-1	
Fat	1k	2.24e-2	2.41e4	5.98e-2	6.65e-6	2.58e-3	
	10k	2.38e-2	1.09e3	2.53e-2	7.33e-5	8.56e-3	n/a
	100k	2.44e-2	9.29e1	2.11e-2	7.54e-4	2.75e-2	
	1M	2.51e-2	2.72e1	6.03e-2	7.44e-3	8.62e-2	
Dry skin	1k	2.00e-4	1.14e3	3.16e-1	4.32e-8	2.08e-4	2.78e-4
	10k	2.04e-4	1.13e3	3.09	1.34e-6	1.16e-3	2.72e-3
	100k	4.51e-4	1.12e3	1.38e1	1.82e-4	1.35e-2	1.23e-2
	1M	1.32e-2	9.91e2	4.16	1.32e-2	1.15e-1	4.20e-3
Wet skin	1k	6.60e-4	3.20e4	2.69	3.57e-7	5.94e-4	8.42e-5
	10k	2.90e-3	2.90e4	5.56	4.17e-5	6.46e-3	1.92e-4
	100k	6.60e-2	1.50e4	1.26	5.48e-4	2.34e-2	8.42e-5
	1M	2.20e-1	1.80e3	4.55e-1	3.78e-2	1.95e-1	2.53e-4

can be expressed as

$$V_s(r,\phi,z) = \sum_{m=1}^{\infty}\sum_{n=0}^{\infty}\left[E_{smn}I_n\left(\frac{m\pi r}{h}\right)\cos(n\phi) + F_{smn}I_n\left(\frac{m\pi r}{h}\right)\sin(n\phi) + G_{smn}K_n\left(\frac{m\pi r}{h}\right)\cos(n\phi) + H_{smn}K_n\left(\frac{m\pi r}{h}\right)\sin(n\phi)\right]\sin\left(\frac{m\pi z}{h}\right) \quad (13)$$

where I_n is the modified Bessel function of the first kind of order n and K_n is the modified Bessel function of the second kind of order n.

Enforcement of (8), (11), and (12), and the constants E_{smn}, F_{smn}, G_{smn}, and H_{smn} in (13) can then be found by using (14) and (15). Since V is finite at $r = 0$, G_{1mn} and H_{1mn} are equal to zero for the innermost tissue

$$A\begin{bmatrix} E_{Nmn} \\ G_{Nmn} \\ E_{N-1mn} \\ G_{N-1mn} \\ \vdots \\ E_{1mn} \end{bmatrix} = \begin{bmatrix} \alpha_1 \\ 0 \\ 0 \\ 0 \\ \vdots \\ 0 \end{bmatrix} \quad (14)$$

$$B\begin{bmatrix} F_{Nmn} \\ H_{Nmn} \\ F_{N-1mn} \\ H_{N-1mn} \\ \vdots \\ F_{1mn} \end{bmatrix} = \begin{bmatrix} \alpha_2 \\ 0 \\ 0 \\ 0 \\ \vdots \\ 0 \end{bmatrix} \quad (15)$$

where

$$k_m = \frac{m\pi}{h} \quad (16)$$

$$a_n = \begin{cases} 2\pi, & \text{for } n = 0 \\ \pi, & \text{otherwise} \end{cases} \quad (17)$$

$$\gamma_s = \sigma_{\mathrm{Eq(s)}} = \sigma_s + j\omega\epsilon_{rs}\epsilon_0 \quad (18)$$

$$\alpha_1 = \frac{2}{h}\int_{-\pi}^{\pi}\int_0^h J_n(\phi,z)\sin\left(\frac{m\pi z}{h}\right)\cos(n\phi)dzd\phi \quad (19)$$

$$\alpha_2 = \frac{2}{h}\int_{-\pi}^{\pi}\int_0^h J_n(\phi,z)\sin\left(\frac{m\pi z}{h}\right)\sin(n\phi)dzd\phi \quad (20)$$

A and *B* are shown at the bottom of the next page, and $[*]'$ indicates the first derivative of the argument.

III. *In Vitro* EXPERIMENT

An *in vitro* experiment, which is designed to suppress the uncertainties arising from the variations of the human body in *in vivo* experiment, is conducted to validate the proposed mathematical model. Inspired by the work of Hackisuka *et al.* in [22], Shinagawa *et al.* in [23], and Fujii *et al.* in [13] and [24], a two-layer phantom with 150 mm (radius of the inner layer is 100 mm) in radius and 500 mm in length is constructed (as shown in Fig. 2). The conductivity and relative permittivity of the material of the outer layer (composition: agar 1 g, sucrose 1 g, and water 0.1 L) are 0.01 S/m and 96, respectively. While, for the inner layer (composition: agar 1 g, potassium dihydrogen phosphate 0.02 g, and water 0.1 L) are 0.034 S/m and 93, respectively.

To build the two-layer phantom for the *in vitro* experiment, first, the mixture of the outer layer material was boiled and

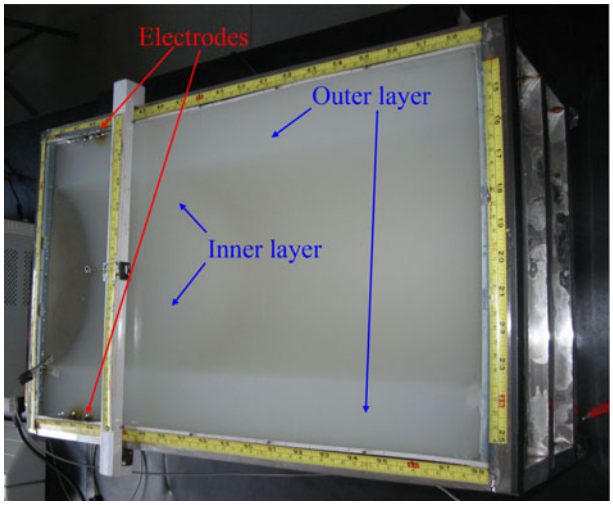

Fig. 2. Experiment setup for the *in vitro* experiment.

poured into the mold. After the outer layer was completely solidified, the melted inner layer material was added. Then, two 10-mm-width ring-type transmitter electrodes were placed on the lateral surface of the phantom cylinder, located 50 and 70 mm away from the end of the cylinder. This implies that the electrical signal applied to the phantom is

$$J_n(\phi, z) = \begin{cases} -J, & \text{if } 50 \text{ mm} < z < 60 \text{ mm} \\ J, & \text{if } 70 \text{ mm} < z < 80 \text{ mm} \\ 0, & \text{Otherwise} \end{cases}$$
$$0 < \phi < 2\pi. \qquad (21)$$

By applying the electrical signal (30 kHz sinusoidal wave) to the transmitter electrodes, the voltage within the phantom was spatially measured and compared with the calculated results from the proposed mathematical model. Fig. 3 shows the results both on the surface and 70 mm deep in the phantom along the z-direction. In comparison with the measurement and calculation results, the maximum error is less than 10%. Measurements along the r-direction on $z = 110$ mm and $z = 280$ mm are also shown in Fig. 4. The experiment results are close to the calculation results and fall within 10% error.

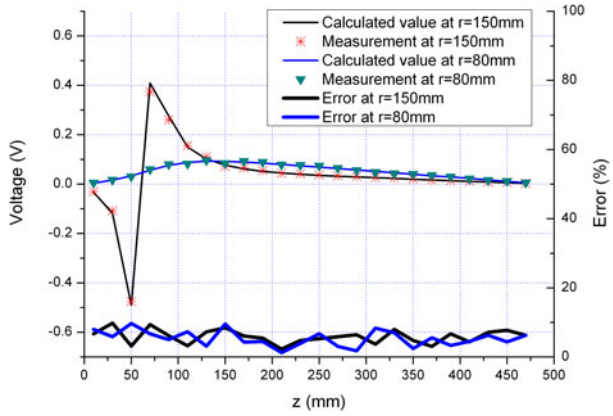

Fig. 3. Comparison of the measured and the calculated results in the z-direction of the phantom.

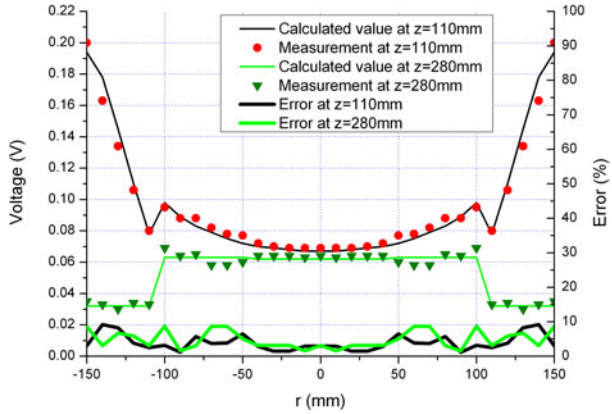

Fig. 4. Comparison of the measured and the calculated results in the r-direction of the phantom.

$$A = \begin{bmatrix} \gamma_N a_n[I_n(k_m r_N)]' & \gamma_N a_n[K_n(k_m r_N)]' & 0 & 0 & \dots & 0 \\ I_n(k_m r_s) & K_n(k_m r_s) & -I_n(k_m r_s) & -K_n(k_m r_s) & \dots & 0 \\ \gamma_{s+1}[I_n(k_m r_s)]' & \gamma_{s+1}[K_n(k_m r_s)]' & -\gamma_s[I_n(k_m r_s)]' & -\gamma_s[K_n(k_m r_s)]' & \dots & 0 \\ \vdots & \vdots & \vdots & \vdots & \ddots & \vdots \\ 0 & 0 & 0 & I_n(k_m r_1) & K_n(k_m r_1) & -I_n(k_m r_1) \\ 0 & 0 & 0 & \gamma_2[I_n(k_m r_1)]' & \gamma_2[K_n(k_m r_1)]' & -\gamma_1[I_n(k_m r_1)]' \end{bmatrix}$$
$$\text{for } n = 0 \dots \infty$$

$$B = \begin{bmatrix} \gamma_N \pi[I_n(k_m r_N)]' & \gamma_N \pi[K_n(k_m r_N)]' & 0 & 0 & \dots & 0 \\ I_n(k_m r_s) & K_n(k_m r_s) & -I_n(k_m r_s) & -K_n(k_m r_s) & \dots & 0 \\ \gamma_{s+1}[I_n(k_m r_s)]' & \gamma_{s+1}[K_n(k_m r_s)]' & -\gamma_s[I_n(k_m r_s)]' & -\gamma_s[K_n(k_m r_s)]' & \dots & 0 \\ \vdots & \vdots & \vdots & \vdots & \ddots & \vdots \\ 0 & 0 & 0 & I_n(k_m r_1) & K_n(k_m r_1) & -I_n(k_m r_1) \\ 0 & 0 & 0 & \gamma_2[I_n(k_m r_1)]' & \gamma_2[K_n(k_m r_1)]' & -\gamma_1[I_n(k_m r_1)]' \end{bmatrix}$$
$$\text{for } n = 1 \dots \infty$$

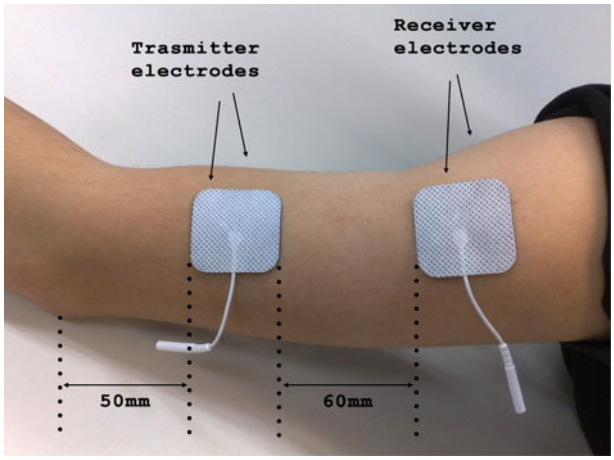

Fig. 5. Placement of the electrodes in the experiment (not to scale).

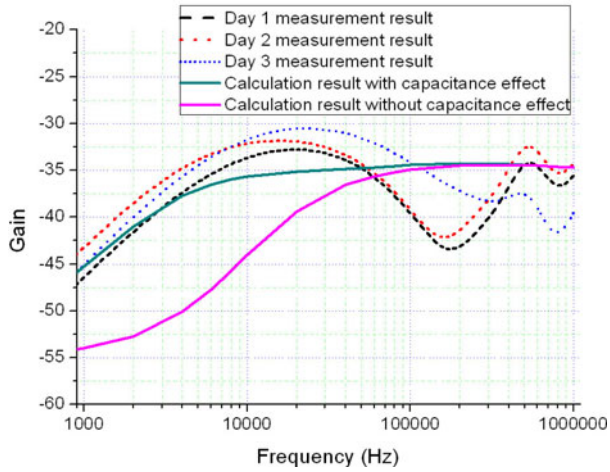

Fig. 6. Results of the measurement data and the calculations.

In our *in vitro* experiment, the major sources of error came from the imperfect manufacturing of the phantom and measurement error. From observation, it was apparent that a slight deformation of the phantom occurs due to the weight of the constituted materials and due to dehydration on the surface. In addition, precise positioning of the measuring probe into the phantom is difficult to achieve, and therefore, error can be expected when comparing experimental result with calculation.

IV. *In Vivo* Experiment

For further evaluation, *in vivo* experiments were also conducted to compare the calculations with the mathematical model. A healthy 26-year-old male subject was chosen and the geometrical data of subject's upper arm were 250 mm in length and 65 mm in diameter on average. Stimulating electrodes (40 mm $\times$ 40 mm) were chosen to apply the transmitted signal into the human body and retrieve the signal. The transmitter electrodes were placed 50 mm away from the elbow and laterally oriented on the upper limb. The receiver electrodes were attached 60 mm away from the edge of the transmitter electrodes. The detailed arrangement can be found in Fig. 5.

The calculation of the voltage distribution was obtained in (13). First, constants in the equation were obtained by evaluating (19) and (20) with the transmitted signal. In the case of our IBC arrangement, J_n is defined as

$$J_n(\phi, z) = \begin{cases} J, & \text{if } -0.615 < \phi < 0.615 \\ -J, & \text{if } \pi - 0.615 < \phi < \pi + 0.615 \\ 0, & \text{Otherwise} \end{cases}$$
$$50 \text{ mm} \leq z \leq 90 \text{ mm} \tag{22}$$

where J is the normal component of the current density.

In this research, four layers of tissue, namely, bone, muscle, fat, and skin are considered. Eventually, the distribution of voltage is computed and the channel gain can, then, be evaluated. In Fig. 6, the calculated results for the model with and without the capacitance effect are plotted. In comparison with the model neglecting the capacitance effect, the model considering the capacitance effect has a higher gain below 100 kHz, while the two models have similar gains at high frequencies. This observation is matched with the quasi-static criteria check for wet skin in Table I, where the capacitance effect of wet skin is less significant at high frequency, such as 1 MHz.

Measurements on the human subject were done for three days in order to validate the calculated results of the mathematical model. A calibrated Agilent 4395A Network/Spectrum/Impedance analyzer was used to measure the channel gain of the IBC on the upper arm of the subject with testing frequency spanning from 1 kHz to 1 MHz. Before the experiment, the skin of the subject was prepared to ensure good contact with the electrodes. Additionally, the transfer characteristic of the measurement setup is taken as the baseline for later compensation. The measurement results (three days) can be found in Fig. 6 and they are consistent except for on day 2 and at higher frequencies. From the analyses, we found that the maximum errors between measurements and calculations with capacitance effect were about 5 dB (at 40 kHz) for operating frequency less than 100 kHz and about 11 dB (at 170 kHz) for operating frequency over 100 kHz. The major causes of error remain vague, and repeatedly slight inaccurate positioning of the electrodes during experiments, the geometrical approximation of the limb, and variations on subject's physiological status are potential considerations at present. The measurement results also show a peak for channel gain in the range of 10–40 kHz, which suggests a possible optimum operating frequency for the galvanic coupling IBC on human limb below 1 MHz.

V. Result Discussion

The *in vitro* experiment discussed in Section III reduces the intrinsic uncertainties when evaluating the accuracy and capability of the mathematical model. Although slight errors exist, the comparisons between the measurement and calculation results show that the model is matched with the experiment data not only limited to the surface of the phantom, but also the inside of the various tissues. This highlights the inner probing advantage of the *in vitro* over the *in vivo* experiment, in which

measuring subcutaneous voltage is almost impossible. The experiment also shows the possibility of using galvanic coupling IBC for communicating with implantable devices, although the attenuation is higher than those receiving electrodes situated on the surface.

Despite the existence of various uncontrollable factors, the importance of *in vivo* experiment is obvious. A comparison between *in vivo* experiments and calculations can reflect how correct the model is in reality. From the results in Fig. 6, the model agrees with the experimental results. The gain calculated from the proposed model coincides with the measurement results at low frequencies (less than 5 kHz) and the maximum error between the calculation and experimental results is less than 5 dB for operating frequencies below 100 kHz. For operating frequencies higher than 100 kHz, the trend for the calculated result differs slightly from the experimental results and the maximum error is less than 10 dB. It is worth pointing out that the error between the calculated and the measurement result is relatively small, since the variations between three days of experiments are in the same order of magnitude.

From the model and the experiments, we can surmise the path of the major propagating medium of IBC. From (4) and the last column in Table I, the calculated results show that the amount of radiation from the tissue is small and negligible. On the other hand, both the measured and the calculated results show that the gain of IBC is higher than -75 dB, which is the measured gain between the transmitter and the receiver electrodes through air in our experimental setting. Thus, one can conclude that the major propagation path of IBC is the human limb and negligible portion of the propagation over the air exists for operating frequency below 1 MHz.

VI. Conclusion

The IBC is a potential communication methodology for the construction of BAN and BSN in many application areas. Especially in the field of medical instrumentation, it can facilitate efficient data exchange for on-body and in-body devices without hindering daily movement. And, it is also a more natural and convenient way for body-centric communication.

In this paper, the authors attempted to analyze the IBC channel from the prospective of the electromagnetic theory and managed to develop a mathematical model to represent the IBC signal distribution on a upper human arm. By validating the quasi-static criteria over the operating frequency range, it has been found that neglecting the capacitance effect would induce significant error whenever skin is included. Thus, the permittivities of tissues were properly included in our corresponding analytical model.

The accuracy of the developed model was also validated with the *in vitro* and the *in vivo* experiments. Both experimental results showed that the proposed model was good for galvanic coupling type IBC on the human limb. For the *in vitro* experiments, the maximum error between model and calculation was less than 10%; while, the maximum difference between model and *in vivo* experiments was less than 5 dB below 100 kHz. In addition, the analysis of the galvanic coupling type IBC with the electromagnetic theory also provides data to deduce that the major IBC signal was confined within the human body and the body channel was more efficient than the air channel for operating frequencies under 1 MHz. Through our *in vivo* experiments, current configuration demonstrated the feasibility of the galvanic coupling type IBC. And, we can easily transform into an embedded communication module for BAN/BSN.

In the next step, inclusion of the anisotropic characteristics of the human tissue shall be investigated in order to increase the accuracy of the model. Moreover, extending the model to other parts of the human body and investigation on modulating schemes are also worth studying.

References

[1] T. G. Zimmerman, "Personal area networks (pan): Near-field intra-body communication," Ph.D. dissertation, Dept. Archit., Massachusetts Institute of Technology, Cambridge, 1995.

[2] T. G. Zimmerman, "Personal area networks: Near-field intrabody communication," *IBM Syst. J.*, vol. 35, nos. 3–4, pp. 609–617, 1996.

[3] T. Handa, S. Shoji, S. Ike, S. Takeda, and T. Sekiguchi, "A very low-power consumption wireless ECG monitoring system using body as a signal transmission medium," in *Proc. Int. Conf. Solid-State Sens., Actuators.*, 1997, pp. 1003–1006.

[4] K. Hachisuka, A. Nakata, T. Takeda, K. Shiba, K. Sasaki, H. Hosaka, and K. Itao, "Development of wearable intra-body communication devices," *Sens. Actuators A, Phys.*, vol. 105, no. 1, pp. 109–115, 2003.

[5] M. S. Wegmueller, A. Kuhn, J. Froehlich, M. Oberle, N. Felber, K. Kuster, and W. Fichtner, "An attempt to model the human body as a communication channel," *IEEE Trans. Biomed. Eng.*, vol. 54, no. 10, pp. 1851–1857, Oct. 2007.

[6] K. Hachisuka, Y. Terauchi, Y. Kishi, K. Sasaki, T. Hirota, H. Hosaka, K. Fujii, M. Takahashi, and K. Ito, "Simplified circuit modeling and fabrication of intrabody communication devices," *Sens. Actuators A, Phys.*, vol. 130–131, pp. 322–330, 2006.

[7] M. Shinagawa, M. Fukamoto, K. Ochiai, and H. Kyuragi, "A near-field-sensing transceiver for intra-body communication based on the electro-optic effect," in *Proc. 20th IEEE Instrum. Meas. Technol. Conf.*, 2003, vol. 1, pp. 296–301.

[8] D. P. Lindsey, E. L. Mckee, M. L. Hull, and S. M. Howell, "A new technique for transmission of signals from implantable transducers," *IEEE Trans. Biomed. Eng.*, vol. 45, no. 5, pp. 614–619, May 1998.

[9] M. S. Wegmueller, S. Huclova, J. Froehlich, M. Oberle, N. Felber, N. Kuster, and W. Fichtner, "Galvanic coupling enabling wireless implant communications," *IEEE Trans. Instrum. Meas.*, vol. 58, no. 8, pp. 2618–2625, Aug. 2009.

[10] M. Fukomoto, M. Shinagawa, and T. Sugimura, "Body coupled fingering: Wireless wearable keyboard," in *Proc. Conf. Human Factors Comput. Syst.*, 1997, pp. 147–154.

[11] R. Xu, H. Zhu, and J. Yuan, "Characterization and analysis of intra-body communication channel," in *Proc. IEEE Antennas Propag. Soc. Int. Symp.*, 2009, pp. 1–4.

[12] K. Fujii, D. Ishide, M. Takahashi, and K. Ito, "Electric field distributions generated by a wearable device using simplified whole human body models," *Inf. Media Technol.*, vol. 4, no. 2, pp. 647–654, 2008.

[13] K. Fujii, M. Takahashi, and K. Ito, "Electric field distributions of wearable devices using the human body as a transmission channel," *IEEE Trans. Antennas Propag.*, vol. 55, no. 7, pp. 2080–2087, Jul. 2007.

[14] M. S. Wegmueller, M. Oberle, N. Kuster, and W. Fichtner, "From dielectrical properties of human tissue to intra-body communications," in *World Congr. Med. Phys. Biomed. Eng.*, 2006, vol. 14, pp. 613–617.

[15] T. Sasamori, M. Takahashi, and T. Uno, "Transmission mechanism of wearable device for on-body wireless communications," *IEEE Trans. Antennas Propag.*, vol. 57, no. 4, pp. 936–942, Apr. 2009.

[16] J. Oh, J. Park, H. Lee, and S. Nam, "The electrode structure to reduce channel loss for human body communication using human body as transmission medium," in *Proc. IEEE Antennas Propag. Soc. Int. Symp.*, 2007, pp. 1517–1520.

[17] R. Plonsey and E. B. Heppner, "Considerations of quasi-stationarity in electrophysiological systems," *Bull. Math. Biophys.*, vol. 29, pp. 657–664, 1967.

[18] R. Plonsey, "Volume conductor theory," in *The Biomedical Engineering Handbook*, J. D. Bronzino, Ed., 2nd ed. Boca Raton, FL: CRC Press, 2000.
[19] J. Malmivuo and R. Plonsey, *Bioelectromagnetism*. New York: Oxford Univ. Press, 1995.
[20] S. Gabriel, R. W. Lau, and C. Gabriel, "The dielectric properties of biological tissues: III. Parametric models for the dielectric spectrum of tissues," *Phys. Med. Biol.*, vol. 41, pp. 2271–2293, 1996.
[21] J. Larsson, "Electromagnetics from a quasistatic perspective," *Amer. J. Phys.*, vol. 75, no. 3, pp. 230–239, 2007.
[22] K. Hachisuka, A. Nakata, T. Takeda, Y. Terauchi, K. Shiba, K. Sasaki, H. Hosaka, and K. Itao, "Development and performance analysis of an intra-body communication device," in *Proc 12th Int. Conf. Transducers, Solid-State Sens., Actuators, Microsyst.*, 2003, pp. 1722–1725.
[23] M. Shinagawa, M. Fukumoto, K. Ochiai, and H. Kyuragi, "A near-field-sensing transceiver for intrabody communication based on the electroopic effect," *IEEE Trans. Instrum. Meas.*, vol. 53, no. 6, pp. 1533–1538, Dec. 2004.
[24] K. Fujii, M. Takahashi, K. Ito, K. Hachisuka, Y. Terauchi, Y. Kishi, K. Sasaki, and K. Itao, "Study on the transmission mechanism for wearable device using the human body as a transmission channel," *IEICE Trans. Commun.*, vol. E88-B, no. 6, pp. 2401–2410, 2005.

Sio Hang Pun received the Master degree in computer and electrical program from the University of Porto, Porto, Portugal, in 1999. He is currently working toward the Ph.D. degree from the Department of Electrical and Electronics Engineering, Faculty of Science and Technology, University of Macau, Taipa, Macau, China.

Since 2000, he has been involved in research in the areas of biomedical engineering.

Yue Ming Gao received the Ph.D. degree in electrical engineering from Fuzhou University, Fuzhou, China, in 2010.

Since 2004, he has been involved in research in the areas of bioelectromagnetism and detecting technology. He is currently an Assistant Researcher in the College of Physical and Information Engineering, Fuzhou University.

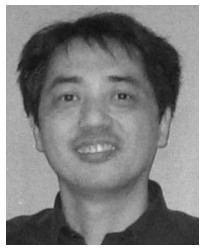

PengUn Mak received the B.Sc. degree from National Taiwan University, Taipei, Taiwan, and the M.Sc. and Ph.D. degrees from Michigan State University, East Lansing, all in electrical engineering.

Since 1997, he has been an Assistant Professor in the Department of Electrical and Electronics Engineering, University of Macau, Taipa, Macau, China. He has authored/coauthored more than 100 peer-reviewed technical publications (journal, book-chapter, conference proceedings etc.) His current research interests include bioelectromagnetism, intra-body communication and bioelectric signals acquisition.

Mang I Vai received the Ph.D. degree in electrical and electronics engineering from the University of Macau, Taipa, Macau, China, in 2002.

Since 1984, he has been involved in research in the areas of digital signal processing and embedded systems. He is currently an Associate Professor and the Head of the Department of Electrical and Electronics Engineering, Faculty of Science and Technology, University of Macau.

Min Du received the Ph.D. degree in Electrical Engineering and Automation from Fuzhou University, Fuzhou, China, in 2005.

Since 1986, she has been involved in research in the areas of biomedical engineering. She is currently a Full Professor in the College of Physical and Information Engineering, Fuzhou University.